2026 IEEE International Conference on Robotics and Automation (ICRA 2026)
June 1-5, 2026. Vienna, Austria

Force-Guided Collaborative Control and Digital Twin of a Snake Robot for Cranial Bone Surgery

Jones Law[1,2*], Camron Sabahi-Pourkashani[1,4*], Liheng Fan[1,3*], Majid Roshanfar[1,2], Kashfia Mahmood[1,2], Adnan Munawar[6], Thomas Looi[1,2], Eric Diller[2,5], and Dale Podolsky[1,2]

***Abstract*— Tendon-driven snake-like robots have demonstrated potential for minimally invasive surgery, particularly in anatomically constrained regions. A previously developed system for cranial bone cutting integrated such a snake robot with an industrial manipulator, yielding a combined 9 degrees-of-freedom (DOF). However, direct operation of a high-DOF system is difficult for a human operator to control. Conventional robotic platforms often rely on teleoperation, which, while effective, physically separates the operator from the surgical site, reducing intuitive control and potentially increasing procedural risk. In this study, we introduce the first system that integrates a force-guided controller with a real-time digital simulator and full-shape virtual fixture (VF) to enhance human–robot interaction in cranial surgery. The controller enables shared autonomy, allowing the surgeon to apply input forces while the robot guides motion along a desired follow-the-leader (FTL) trajectory. The simulator provides synchronized visualization of the physical and virtual environment, offering both surgical planning insight and intraoperative feedback. Experimental results demonstrated that the proposed system facilitates collaborative control. The system shows improved accuracy and stability compared to manual operation, with average errors of 6.79 ± 3.27 mm at the handle and 7.13 ± 1.39 mm at the tool-tip, versus 13.61 ± 3.05 mm without guidance. The results also demonstrate that a 5 N force threshold offers the best balance of responsiveness and stability. Using this system, the robot successfully performed FTL cutting motion on a physical skull model with 2 mm bone thickness.**

I. Introduction

Minimally invasive surgical robots often need to traverse narrow anatomical passages to reach the target sites, presenting significant challenges for motion control and visualization [1]. Unlike trans-abdominal procedures, which are primarily constrained by a remote center of motion, minimally invasive craniotomies (skull or cranial bone cuts) require precise control of the robot's full kinematic shape. For these procedures, the robot must follow a prescribed bone-cutting trajectory on the skull while operating within narrow corridors bounded by soft tissues, including the scalp, dura and brain [2]. Such a system is required to conform to the skull curvature using a minimal access incision with specific application in craniosynostosis (premature skull fusion) surgery.

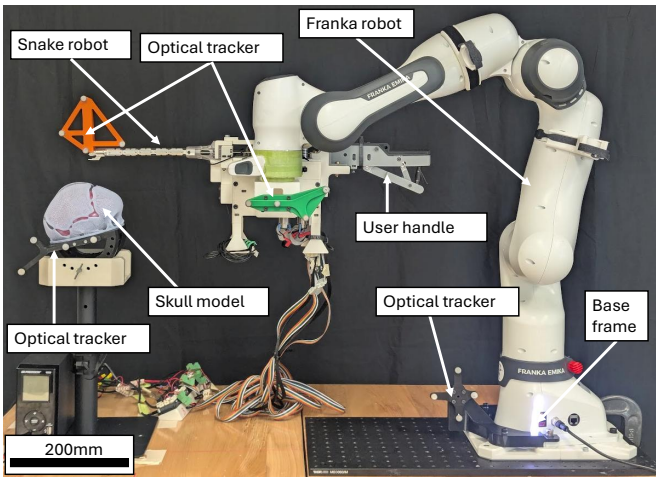

Fig. 1: System overview for cranial bone-cutting experiments: a tendon-driven snake robot is mounted on a Franka manipulator and operates along a 3D skull model. Optical trackers register the Franka base and flange, the skull, and the planned path; a user handle attached at the flange provides measured input forces for the force-guided controller.

Most manual surgical devices focus on the end-effector position and orientation and have only one bending section with the ability to control only one degree-of-freedom (DOF) at a time [3]. Multiple snake-like surgical robots have been developed with mechanisms capable of articulating along curved paths, such as multi-rigid linkage systems and elastic backbone designs [4]. However, these robots focus on teleoperation and automation. As a result, efficient strategies are lacking for controlling the motion and shape of these robots when navigating irregular, curved passages under direct collaborative control by surgeons. This challenge is exemplified by the cranial surgical robotic system we previously developed [5] with multiple bending segments and DOF. In this work, the surgical task is the performance of minimally invasive cranial bone-cuts (craniotomies). Successful robotic navigation for this procedure requires at least 6-DOF to control the end-effector pose, along with additional DOF to manage the robot's overall shape. Efficiently controlling a snake-like robot with multiple bending segments is particularly challenging for human operators, especially when the robot's shape cannot be directly visualized through the endoscopic tool-tip view. Therefore, autonomous assistance is required in addition to direct surgeon input, enabling a collaborative shared-control for safe and accurate navigation.

[1] The Wilfred and Joyce Posluns Centre for Image Guided Innovation and Therapeutic Intervention, The Hospital for Sick Children, Canada.
[2] Institute of Biomedical Engineering, University of Toronto, Canada.
[3] Division of Engineering Science, University of Toronto, Canada.
[4] Department of Mechanical and Mechatronics Engineering, University of Waterloo, Canada.
[5] Microrobotics Laboratory, University of Toronto, Canada.
[6] Laboratory for Computational Sensing and Robotics, Johns Hopkins University, USA.
The first three authors contributed equally to this work. Asterisk indicates corresponding authors.

979-8-3315-8160-2/26/$31.00 ©2026 IEEE

To navigate the geometric constraints encountered during minimally invasive surgery, virtual fixtures (VFs) have been widely investigated. A VF is a software-defined constraint, implemented through haptic forces or position-based guidance that restricts or directs the instrument motion, thereby enhancing both safety and accuracy. This approach has been used in assistance for suturing in robot-aided pediatric endoscopic surgery [6] and cardiac surgery [7]. In collaborative robotic settings, VFs may generate artificial force feedback, modulate the user's applied force [8] [9], or constrain the end-effector motion through velocity admittance or impedance control schemes [10]. Defining VFs in the surgical environment allows for safe cooperative control involving humans and robots [11]. However, although keyhole and surface types VFs have been extensively studied, implementing VFs for full shape of snake-like robots operating through narrow passages continues to be a challenging research problem.

Preoperative motion planning and shared-control are also critical for enabling safe human–robot cooperation and the reliable execution of surgical procedures. By providing surgeons with insight into the robot's motion before and during surgery, surgical planning adds an essential layer of safety. Surgeons have shown increased specific psychomotor skills by practicing on a virtual simulator [12] for laparoscopic surgery, and improved situational awareness [13]. Simulation platforms such as Asynchronous Multi-Body Framework (AMBF) [14], and Unity [15] have been used for surgical simulation and training. However, implementation of shared control and simulation with surgical snake robots remains an open research challenge.

Furthermore, due to the complex kinematic chain of the robotic system, mechanical properties such as backlash and tolerance contribute to the inaccuracy of end-effector position [16]. As a result, many existing surgical robot rely on human-in-the-loop control via teleoperation. This approach physically separates the surgeon from the surgical site, which can diminish operational intuitiveness and delay response during emergencies. From a safety perspective, the surgeon should maintain physical shared-control over the robots instrument motion when navigating complex paths.

There is a need for an assistive system that integrates surgeons' and robot inputs as shared control for a cranial surgical snake robot. In this work, we propose a novel control strategy in which a digital twin simulator is used to generate virtual fixtures (VFs) that regulate end-effector trajectories and robot shape during craniotomies. There are two major contributions of this study: (i) a force-guided controller that enables safe and effective physical human–robot interaction (pHRI) during the performance of craniotomies; (ii) a virtual simulation framework that models both the robotic motion and cutting process on a three-dimensional (3D) skull model. To the best of our knowledge, this is the first system that combines force-guided shared control with a digital twin simulator to generate FTL virtual fixtures for the performance of craniotomies.

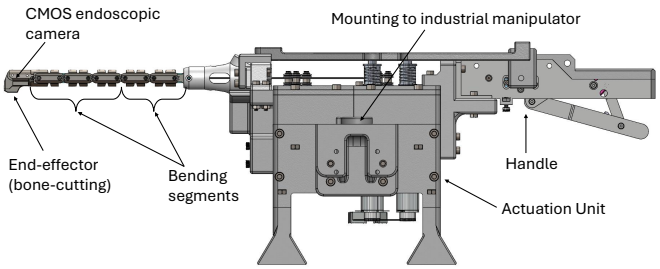

Fig. 2: Overview of the snake robot, which consists of two bending segments actuated by antagonistic tendons. The system integrates a bone-cutting jaw, an endoscope, an actuation unit, and a surgeon physical interface (handle).

II. System Design and Methodology

The robotic system consists of a tendon-driven snake robot and an industrial manipulator for positioning. The snake robot is bio-inspired by limbless vertebrates such as snakes and lizards, where the skeleton provides structural support while muscles generate actuation force. This configuration enables these animals to maneuver through narrow passages and perform force-intensive tasks such as burrowing and capturing prey [17]. Similarly, the robot integrates rigid linkages for structural support and tendons for actuation. Secondly, an FTL algorithm [5] is employed to generate a trajectory for the robot to follow, enabling it to conform to the curvature of the cutting paths on the skull. This trajectory is treated as a VF, where the force guiding algorithm constrains the motion to remain on the trajectory. During operation, the surgeon interacts with the system via a handle, applying forces that are measured by integrated torque sensors. The force inputs are used to guide the robot's advancement along the trajectory. In addition, an endoscope at the end-effector provides real-time visual feedback, allowing the surgeon to fine-tune tip position, ensuring accurate cutting along the target path and preventing unintended contact with surrounding soft tissue. In addition, a virtual simulator was developed for pre-operative analysis and real-time visualization of the cutting progress.

A. Robot Architecture and Mechanical Design

The proposed system integrates a snake robot in series with a 7-DOF industrial manipulator (Franka Research 3, Franka Robotics, Germany) (Fig. 1). The snake robot (Fig. 2) is designed with two actively controlled bending segments (total 175 mm), enabling bending with constant curvature. The distal end-effector incorporates a specialized bone-cutting jaw (punch). In addition, a CMOS-based (Complementary Metal-Oxide-Semiconductor) endoscope (OV6946, Wenqiao Electronics, China) is integrated into the end-effector, providing intraoperative visual feedback. In this study, the cutting tool was designed for planar curved cutting paths, which align with the conventional patterns employed during minimally invasive cranial surgery, such as during an endoscopic strip [2], and extended strip craniectomy [18]. The proximal end of the snake robot is a motorized actuation unit and a handle. This handle is mounted onto the flange of the Franka manipulator, and acts as the physical collaboration interface between the user and the robot.

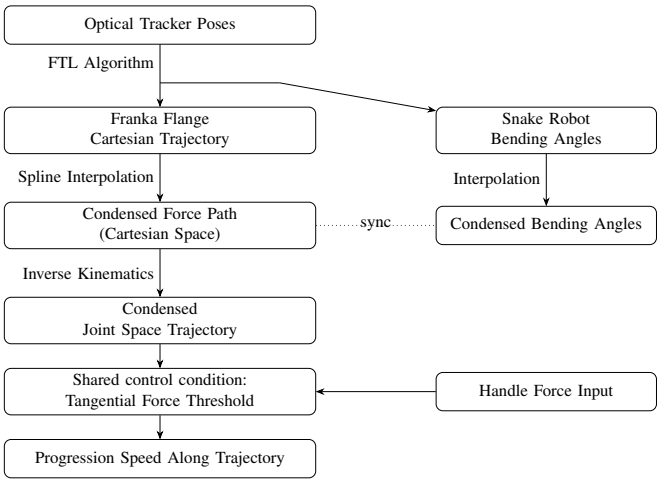

Fig. 3: Workflow of trajectory generation and force-guided execution. Optical tracker poses are converted by the FTL algorithm into a Cartesian trajectory, interpolated and transformed into joint-space commands. User-applied handle forces are filtered by a tangential threshold, while snake robot bending angles are interpolated and synchronized with the flange trajectory.

B. Shared Control with a Virtual Fixture

The shared control algorithm workflow is illustrated in Fig. 3. The desired cutting path is first defined by tracing the skull surface with an optical probe, thereby capturing the desired path as a set of coordinate frames in 3D space using an optical tracker (NDI Polaris Spectra, NDI, Canada). This path is represented as a sequence of discrete coordinate frames, each expressed as a transformation matrix in the special Euclidean group $SE(3)$. In the proposed control strategy, the trajectory is sampled into discrete steps in 3D space (34 in current design). At each step, the configuration space of the snake robot is searched to identify shapes that minimize deviation from the target path [5]. By sequentially linking these configurations, an FTL trajectory is constructed. This trajectory is represented in two components: the Cartesian pose of the Franka flange and the bending angles of the snake robot. Since the user handle is mounted on the force-sensing flange of the Franka robot, the force-guiding calculations only account for the components proximal to the flange.

To ensure smooth motion, the resulting Cartesian trajectory of the Franka flange is interpolated using splines, yielding a dense joint-space path of approximately 5000 points along the trajectory (Condensed Force Path). This corresponds to an average spacing of less than 1 mm between consecutive points. The joint-space trajectory is then calculated using inverse kinematics, which serves as the reference for a force-guided position controller, enabling physical human–robot interaction (pHRI). Simultaneously, the snake robot's bending angle is also interpolated to have the same number of steps as the flange trajectory. The controller, equation (1), interprets force inputs applied by the surgeon at the handle, computes the tangential component of the input relative to the trajectory, and advances the robot along the cutting path in 3D space. Any input force orthogonal to the trajectory is actively rejected, thereby implementing a VF that constrains motion along the predefined path. To further stabilize operation and prevent unintended motion caused by small perturbations, a force threshold is incorporated such that the robot only advances once the applied input exceeds the set threshold. If the tangential force passes the threshold, the Franka robot advances at a constant speed, synchronous with the snake robot motion.

$$\dot{s} \;=\; v_0 H\big(\hat{t}^{\top} F_h - F_{\text{th}}\big), \tag{1}$$

The controller, as described in

$$H(z) = \begin{cases} 1, & z > 0, \\ 0, & z \le 0, \end{cases} \tag{2}$$

where $\dot{s}$ denotes the progression speed along the trajectory; v_0 is the constant progression rate; $\hat{t}$ represents the unit tangent vector at the current point on the trajectory; F_h is the force applied by the surgeon at the robot handle; F_{th} is the threshold force required to initiate motion; and $H(z)$ represents a Heaviside step function.

C. Digital Twin and Simulator Implementation

The digital twin framework workflow is illustrated in figure 4, which consists of both physical and simulation robots. The simulation environment is implemented using AMBF which interfaces with the control system via Robot Operating System (ROS) and supports both joint-level and Cartesian-level operation. In joint-level mode, the controller communicates directly with AMBF, publishing commands independently to each joint (combined snake robot and Franka manipulator). The Cartesian-level mode controls the pose of the Franka flange. To simulate bone cutting, a 3D voxel-based model of the skull is imported to the simulator, similar to [19]. Upon initialization, a collision detection and voxel editing module is activated, generating a dynamic proxy sphere at the robot's end-effector tip to represent its interaction region. This module continuously detects collisions between the proxy sphere and the surrounding voxels. During each physics update, voxels in contact with the sphere are identified and removed; the graphics update step then reflects these changes visually. As a result, the skull model appears to

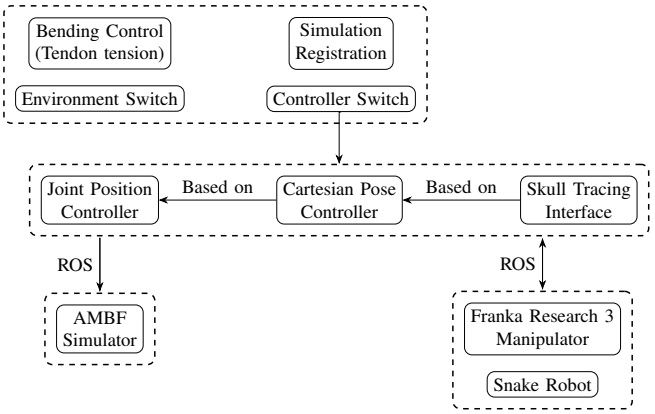

Fig. 4: Overview of the digital twin control framework. The GUI manages bending control, simulation registration, and controller selection. Commands from joint, Cartesian, or skull-tracing controllers are sent via ROS to both the AMBF simulator and the physical system (Franka manipulator and snake robot) for synchronized execution and monitoring.

be "cut" in the simulation as the robot's end-effector follows its programmed path. During simulated surgical procedures, the simulator subscribes to joint commands generated by the FTL algorithm. Using a digital twin framework, the simulation environment maintains a synchronized virtual representation of the physical robot. The robot can operate in either autonomous or shared-control mode. In autonomous mode, the robot is commanded to sequentially reach each point along a predefined trajectory. In shared-control mode, the joint position controller publishes joint command to both physical and virtual robot. This digital twin enables real-time monitoring and control of both robot kinematics and surgical interaction with the voxel-based skull model. All controllers can also be executed independently within the simulation without the physical robot, which allows for validation of algorithms and cutting strategies in a virtual environment.

D. User Interface and Workflow

The overall workflow of the surgical procedure is presented in three stages: registration, pre-operative planning, and digital twin execution. For the registration stage, four optical trackers are first employed to register the spatial relationship between system components: (1) the base of the Franka robot, (2) the flange of the Franka robot, (3) the skull position, and (4) the cutting path along the skull. An additional tracker (Fig. 5) is mounted at the tip of the end-effector to record its trajectory for the following experiments. During pre-operative planning, the cutting path data is imported into the FTL algorithm, which generates the trajectory and corresponding joint-space motion. The resulting motion can be visualized in the simulator, enabling the user to examine the trajectory of the handle, assess safety, and repeat the path-tracing procedure if necessary.

Once validated, the simulator is reset and the digital twin mode is activated, synchronizing the simulator with the physical robot. During operation, the surgeon applies forces to the Franka robot's flange via a handle. When the tangential component of the applied force exceeds a predefined threshold, the robot advances along the planned trajectory. Conversely, non-tangential forces are resisted, thereby constraining motion and guiding the user to apply inputs consistent with the desired cutting path. Throughout the procedure, the simulator provides real-time visualization of the cutting progress. At the same time, endoscopic visual feedback enables the surgeon to fine-tune the end-effector position. This ensures precise alignment of the bone-cutting jaws with the target tissue. The cutting procedure is executed by advancing the robot along the trajectory, with the option to reverse motion and retreat if bone debris becomes trapped in the jaws or if the endoscopic view becomes obstructed.

III. Experimental Validation and Results

To evaluate the performance and reliability of the proposed shared-control framework, a series of experiments were conducted, including (A) system kinematic accuracy, (B) force-guided shared control evaluation, and (C) comparative testing with a physical and digital simulator.

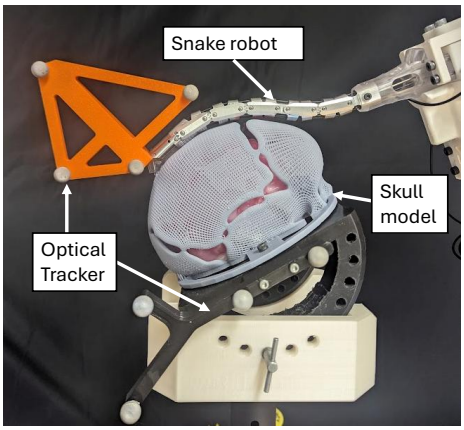

Fig. 5: Snake robot conforming to the curvature of the skull model along the FTL trajectory, reducing deviation and minimizing interference with surrounding soft tissue.

A. System Kinematic Accuracy Test

In this experiment, three optical probes were implemented to track the base and flange coordinate frames of the Franka robot, and tip of the snake robot. The positions and orientations of these probes were recorded using an NDI optical tracker. A sagittal craniosynostosis skull model was used to simulate the bone-cutting procedure. The model was fabricated using a 3D printer (Photon M3 Max, Anycubic, Hong Kong) with a semi-rigid material (Standard Resin, Anycubic, Hong Kong) to replicate the geometry. The skull model was fabricated with a channel that represents the intended cutting trajectory, providing a constrained pathway for the jaw to follow. The integrated system was then commanded to perform the FTL motion under the proposed force-guided controller. During execution, both the snake robot tip and the Franka flange were tracked, and their trajectories were compared against the commanded path. Each test was repeated five times.

Figure 5 demonstrates the FTL algorithms ability to enable the snake robot to conform to the curvature of the skull-cutting path, thereby reducing interference with surrounding tissue. Figure 6a and 6c further illustrates the performance of the force-guided controller: the force sensing flange followed the desired trajectory with an average positional deviation of 6.79 ± 3.27 mm, and the axis-wise deviation profiles along the path progress are presented. The pose of the flange is determined using the FTL algorithm to ensure the snake robot maintains a pose that is suitable for FTL motion while simultaneously avoiding unwanted potential collisions with surrounding anatomy such as the scalp and brain. Table I presents the average positional difference between the commanded and actual trajectories of both the cutting tip and the flange relative to the desired cutting path. Figure 6b presents the tracked tip position of the snake robot. While the robot was commanded to reach specific poses, deviations from the intended path were observed. Figure 6d further demonstrates the axis-wise positional deviation profiles. These deviations are attributed to mechanical factors such as hysteresis, backlash, compliance, and external forces. For bone-cutting applications, interaction forces from the

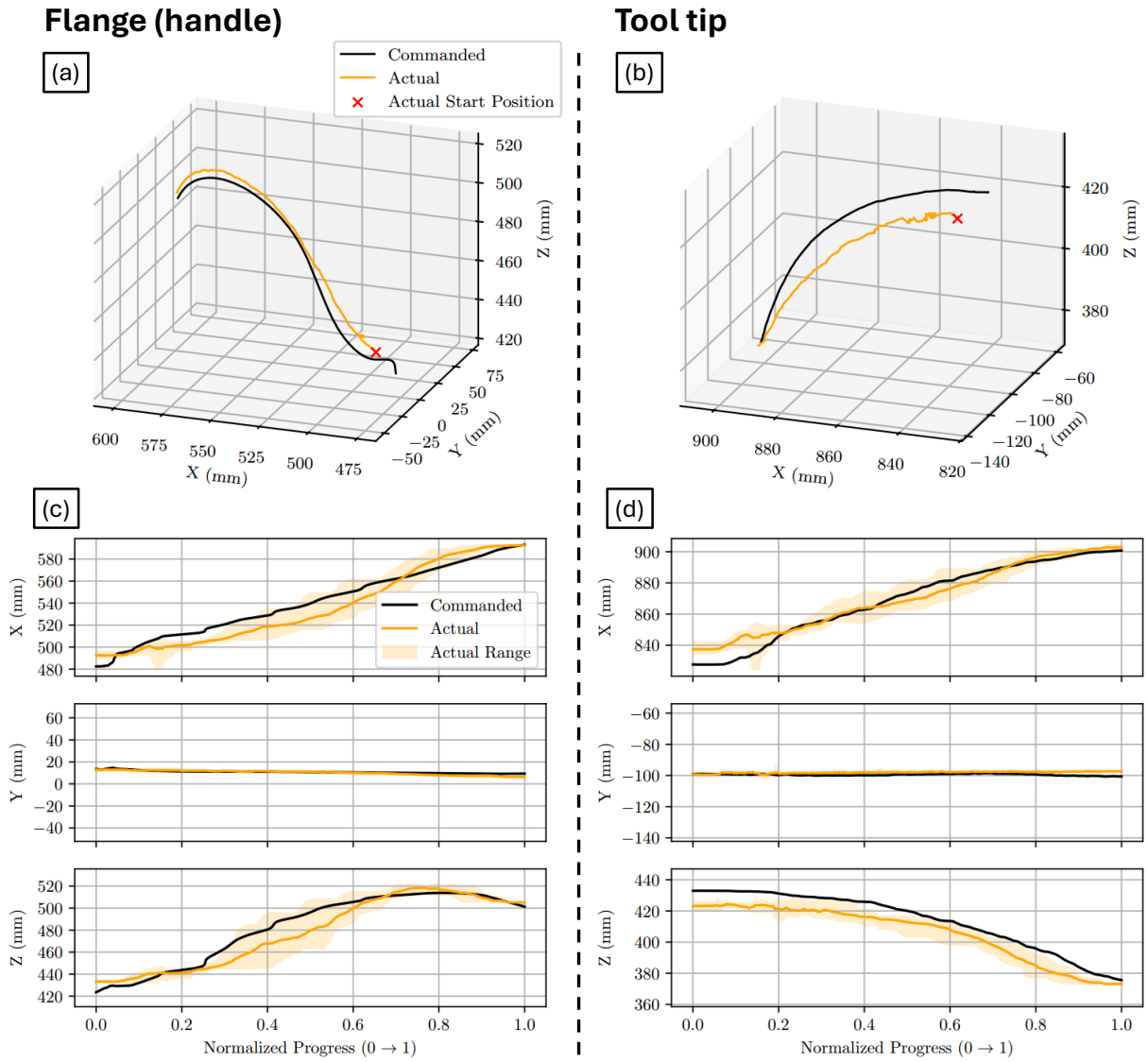

Fig. 6: Comparison of the Franka flange and the snake robots actual trajectory versus the desired FTL trajectory. 3D spatial plot illustrating close alignment with minimal deviation of (a) the flange, (b) snake tool-tip. Axis-wise deviation profiles along the trajectory, illustrating the magnitude and distribution of tracking errors in each direction for (c) the flange, (b) snake tool-tip. These results demonstrate the path accuracy of the force-guided controller.

bone and surrounding tissue further affect the robot's shape and, therefore, its tip position. This result highlights the importance of incorporating human-in-the-loop strategies for ensuring precision and safety. The discrepancies of the tool-tip can also be visualized through the embedded endoscopic view, enabling the operator to compensate in real time by adjusting the distal bending of the snake robot.

TABLE I: Comparison of the positional error between the commanded and actual trajectories of the Franka robot flange and the snake robot tip.

Positional error (mm)	Franka flange, handle	Snake robot tip
Average	6.79 ± 3.27	7.13 ± 1.39
Maximum	17.30 ± 2.40	16.59 ± 2.06

B. Force Guided Shared Control Evaluation

The experimental setup is similar to the system accuracy test and was conducted in four stages. (1) Continuous motion: the user was instructed to trace a trajectory through fabricated channels in a skull model while continuously operating the force-guided controller without pausing. During this process, the interaction forces applied by the user were recorded throughout the skull-tracing motion. (2) Interruption with misaligned force: the user intentionally interrupted the procedure midway and applied external forces in directions misaligned with the intended path to evaluate the system's ability to guide the user back toward the desired trajectory. For both the first and second stages, the tangential input force threshold was set to 5 N, and each experiment was repeated five times. (3) Force threshold evaluation: the influence of varying the threshold value was systematically investigated, where the threshold values of 1, 3, 5, 10, and 15 N were tested. (4) The force guiding is disabled and the Franka robot provided only weight compensation for the bone-cutting tool, while the bending section of the snake robot was manually controlled by the user. In this test, the path deviation and the time required to complete the FTL motion were recorded.

1) Continuous motion: The user attempts to move the robot through the path continuously under force guidance.

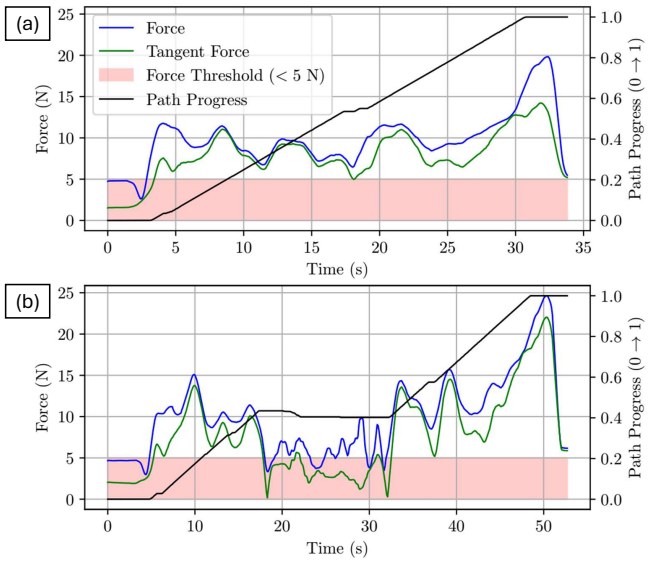

Fig. 7: Comparison of total user-applied force and tangential force with robot motion progress along the trajectory under force-guided control for two scenarios: (a) continuous motion, and (b) intentional pauses and misaligned force applied midway through the trajectory.

The Franka flange motion is tracked, while force sensor readings are collected simultaneously. For each trial, the total applied force, its projection onto the intended path, and the percentage progression along the trajectory were computed. Figure 7a presents the results of one of the five trials in which the user attempted to complete the trajectory without pausing. The trajectory progression plots indicate that when the tangential force component exceeded the prescribed threshold (5 N), the control system permitted advancement along the cutting path at a constant speed along the path. All five trials demonstrate consistent behavior.

2) Interruption with misaligned force: Figure 7b illustrates the scenario where the user deliberately applied forces that are misaligned with the trajectory. The flat region of the black line corresponds to instances where the tangential component of the input force is below the threshold. In such cases, the control system resisted any misaligned force and prevented further progress until the tangential force surpassed the threshold, at which point the trajectory execution resumed. This demonstrates the ability of the system to guide the user to apply forces aligned with the desired path.

3) Force threshold evaluation: To further characterize the effect of the threshold, the experiment was repeated for force thresholds ranging from 1 N to 15 N. Each threshold condition was tested in three trials. Table II summarizes the average completion time and number of pauses to search for the correct path. Furthermore, if the input force from the user to the Franka robot is too high, a safety limit will be triggered and the robot will require a reset. The number of force limits triggered at each threshold level were recorded. At lower thresholds (1 and 3 N), the robot advanced relatively quicker; however, the reduced threshold allowed the robot to advance even when the applied force was misaligned. This often caused the user to continue pushing in the wrong direction, ultimately triggering the safety force limit of the

TABLE II: Effect of varying level of force threshold.

Threshold (N)	Time (s)	No. of Pauses	Safety limit trigger
1	45.5	3.5	1
3	50	4.7	2
5	44.3	2.6	0
10	72	9	0
15	112.5	9.5	3

Franka robot. At higher thresholds (10 and 15 N), the user experienced greater resistance, making it more difficult to maintain high tangential forces along the trajectory. As a result, the completion time increased, and the likelihood of triggering the safety limit also increased due to the higher input forces required. Among the tested values, a threshold of 5 N provided the most balanced performance: the trajectory was completed with minimal pauses, in the shortest overall time, and without triggering the safety limit.

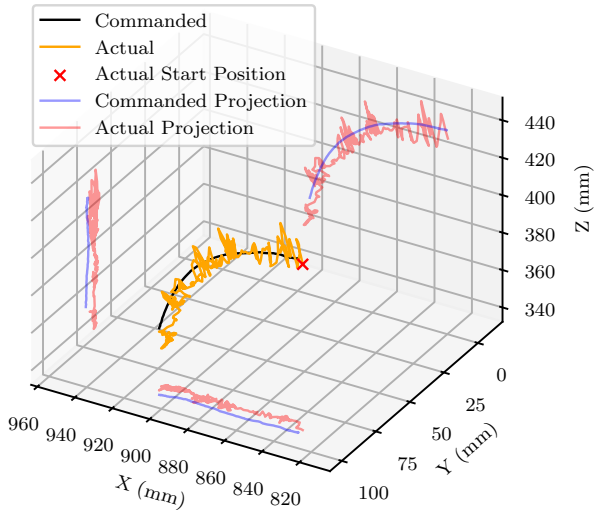

Fig. 8: Snake robot tip trajectory compared with the desired path under manual control without force guidance. Significant deviations and oscillations are observed, highlighting the difficulty of control without VF assistance.

4) No force-guidance: In this test, the force-guiding function was disabled, and the robot was manually operated by the user. As shown in figure 8, under these conditions the robot tip was unable to reliably follow the intended path and frequently deviated, with an average displacement of 13.61 ± 3.05 mm. The tool-tip trajectory exhibited oscillations around the desired path with a maximum deviation of 25.27 ± 5.86 mm, which could pose a risk of damaging surrounding soft tissue. Although the tip eventually reached the end of the path despite substantial oscillations, the user was unable to appropriately adjust the robot shape to perform FTL motion due to the lack of visual feedback. As a result, the snake robot body deviated from the skull curvature, further increasing the likelihood of injury to surrounding tissue.

C. Comparison of Physical and Digital Simulation Cutting

In this experiment, the user performed skull tracing and bone cutting (craniotomies) on a 3D-printed skull model using the force-guided controller. The physical robot and the virtual simulator were deployed in parallel as digital twins.

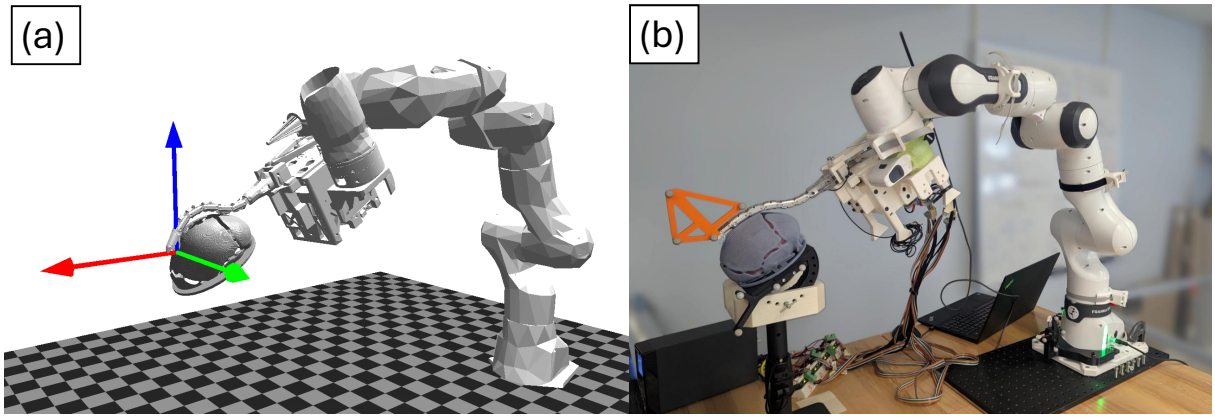

Fig. 9: Digital twin demonstration illustrating synchronized views of the simulator and the physical system from identical viewing angles. The simulator reproduces the kinematics of the physical robot and skull model in real time, allowing the user to visualize and compare execution between the virtual and physical environments. This synchronization enables preoperative trajectory validation and intraoperative monitoring of the craniotomy procedures.

For this experiment, the robot was required to execute the osteotomy on the 3D model that comprised of a skull with a thickness of 2 mm. The simulator was used pre-operatively to provide the user with insight into the planned trajectory and to visualize cutting progress in real time. The simulator also reproduces the kinematics of the physical system, with both the robot and the skull imported into a virtual environment. The virtual robot is commanded to follow the trajectory concurrently with the operation of the physical system. Figure 9 illustrates the synchronized views of the simulator and the physical system from identical viewing angles. The results of the cutting between the physical and simulated system are presented in Fig. 10. The physical cutting path deviated from the virtual model by approximately 5 mm due to reaction forces from the bone acting on the snake robot during cutting, which displaced the tip position. The tip deviation is monitored through the endoscopic view, and user can apply manual correction if needed.

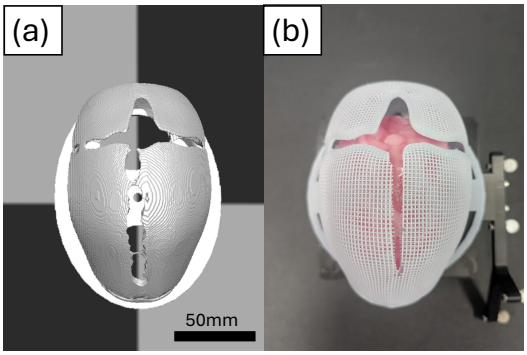

Fig. 10: Comparison of skull cutting results using the simulator (a) and physical (b) robot. The close alignment of outcomes demonstrates the digital twin's ability to replicate physical performance for planning and guidance.

IV. Discussion and Conclusion

This study demonstrates the feasibility of a shared-control framework that integrates force-guided control with digital twin simulation for the performance of craniotomies. The system enables collaborative execution of FTL trajectories, constraining user deviations through virtual fixtures, and provides synchronized visualization to support preoperative planning and intraoperative guidance. Besides validating functionality, the results also highlight limitations and design trade-offs that must be addressed for clinical translation.

A. Limitations and Engineering Considerations

The primary limitation of the current system is positional inaccuracy at the snake robot tip, largely attributable to mechanical backlash, structural deformation, and the absence of task-space sensing on both the Franka and snake robot. Although surgeons can compensate for these errors through visual feedback, reducing backlash and incorporating closed-loop control would minimize the need for manual correction. Similarly, reliance on joint-space data restricts simulator fidelity, contributing to discrepancies between simulated and experimental outcomes. Integrating shape-sensing devices such as Fiber Bragg Grating (FBG) [20] or magnetic sensors [21], as well as task-space tracking at the Franka flange, would enhance both accuracy and simulation reliability. Furthermore, bone punch tools introduce unintended external forces that destabilized the trajectory. Energy-based cutters, such as ultrasonic burrs, may provide more consistent interaction with bone while reducing disturbance forces.

Control design choices also involve trade-offs. First, the present force-guiding approach relies on a threshold-based mechanism to control robot advancement along a fixed trajectory at a constant speed. This is an effective method but provides less transparency and control to the operator. More advanced strategies, such as generating resistance force by artificial potential field or implementing admittance control, could provide more intuitive and collaborative interaction. However, these methods also increase system complexity and computational demands. Secondly, the user's force input only controls the flange motion, while the snake robot bending is governed by interpolation and synchronization. As a result, the cutting speed must be kept sufficiently slow to maintain synchronization. This limitation is acceptable for the current bone punch, since it is a slow instrument that advances less than 5 mm per cut. However, for future developments involving higher-speed cutting tools, the synchronization between the snake robot and the manipulator will need to be controlled via the shape-sensing devices mentioned above.

B. Clinical Translation Considerations

The findings in this work reinforce that force-guided shared control is particularly valuable in constrained surgical environments where tip instability or manipulator deviations could damage adjacent tissues. The threshold for a force guiding system is critical. In this study, 5 N offered the most balanced performance, but the optimal setting will vary for different manipulators and surgical contexts. Calibration may therefore be necessary for different robotic systems and surgical procedures. The digital twin simulator also demonstrates potential for clinical use, providing synchronized visualization and preoperative planning. To be clinically viable, the virtual simulator must be extended to support complex surgical workflows, including multi-path and soft-tissue interaction, while maintaining a clear user interface. Furthermore, adding suction-irrigation features for cleaning debris would be beneficial to the clinical workflow.

C. Future Work

Future development will proceed along three directions. First, improving system accuracy includes refining fabrication tolerances, implementing closed-loop feedback to provide reliable position control, and integrating shape-sensing technologies to reconstruct the full manipulator shape. These improvements will reduce reliance on manual correction.

Second, advanced force-guiding strategies will be investigated. Adaptive force-guiding approaches, admittance control and human-robot negotiation [22] will be explored to provide more intuitive interaction between surgeon and robot. Such strategies allow the operator not only to remain in control of direction but also to modulate speed.

Third, the digital twin simulator will be expanded to support more complex surgical scenarios. This includes handling multi-trajectory planning for extensive osteotomies and integrating deformable environments to model interaction with soft tissue in addition to bone. Enhancing the digital simulator would improve its utility for both preoperative planning and intraoperative adaptation, providing surgeons with more comprehensive support.

In addition to technical directions, user-in-the-loop studies under surgical conditions will be essential to validate the system's performance, usability, and safety. Such evaluations will provide critical insights into workflow integration, ergonomics, and the clinical value of shared-control strategies.

REFERENCES

[1] P. E. Dupont, B. J. Nelson, M. Goldfarb, B. Hannaford, A. Menciassi, M. K. O'Malley, N. Simaan, P. Valdastri, and G.-Z. Yang, "A decade retrospective of medical robotics research from 2010 to 2020," *Science robotics*, vol. 6, no. 60, p. eabi8017, 2021.

[2] C. B. Garland, L. Camison, S. M. Dong, R. S. Mai, J. E. Losee, and J. A. Goldstein, "Variability in minimally invasive surgery for sagittal craniosynostosis," *Journal of Craniofacial Surgery*, vol. 29, no. 1, pp. 14–20, 2018.

[3] P. L. Anderson, R. A. Lathrop, and I. Webster, R. J., "Robot-like dexterity without computers and motors: a review of hand-held laparoscopic instruments with wrist-like tip articulation," *Expert Review of Medical Devices*, vol. 13, no. 7, pp. 661–672, 2016.

[4] J. Seetohul and M. Shafiee, "Snake robots for surgical applications: A review," *Robotics*, vol. 11, no. 3, p. 57, 2022.

[5] J. Law, E. Stickley, R. Gondokaryono, T. Looi, E. Diller, and D. Podolsky, "Design and implementation of a snake robot for cranial surgery," in *2025 IEEE International Conference on Robotics and Automation (ICRA)*. Atlanta, GA, USA: IEEE, 2025, pp. 831–837.

[6] M. M. Marinho, H. Ishida, K. Harada, K. Deie, and M. Mitsuishi, "Virtual fixture assistance for suturing in robot-aided pediatric endoscopic surgery," *IEEE Robotics and Automation Letters*, vol. 5, no. 2, pp. 524–531, 2020.

[7] S. Park, R. D. Howe, and D. F. Torchiana, "Virtual fixtures for robotic cardiac surgery," in *Medical Image Computing and Computer-Assisted Intervention – MICCAI 2001*, W. J. Niessen and M. A. Viergever, Eds. Berlin, Heidelberg: Springer Berlin Heidelberg, 2001, pp. 1419–1420.

[8] H. Ishida, M. Sahu, A. Munawar, N. Nagururu, D. Galaiya, P. Kazanzides, F. X. Creighton, and R. H. Taylor, "Haptic-assisted collaborative robot framework for improved situational awareness in skull base surgery," in *2024 IEEE International Conference on Robotics and Automation (ICRA)*, 2024, pp. 3588–3594.

[9] S. Payandeh and Z. Stanisic, "On application of virtual fixtures as an aid for telemanipulation and training," in *Proceedings 10th Symposium on Haptic Interfaces for Virtual Environment and Teleoperator Systems. HAPTICS 2002*, 2002, pp. 18–23.

[10] D. Hennekens, D. Constantinescu, and M. Steinbuch, "Continuous impulsive force controller for forbidden-region virtual fixtures," in *2008 IEEE International Conference on Robotics and Automation*, 2008, pp. 2890–2895.

[11] Y. He, Y. Hu, P. Zhang, B. Zhao, X. Qi, and J. Zhang, "Human–robot cooperative control based on virtual fixture in robot-assisted endoscopic sinus surgery," *Applied Sciences*, vol. 9, no. 8, p. 1659, 2019.

[12] R. Moldovanu, E. Târcoveanu, G. Dimofte, C. Lupaşcu, and C. Bradea, "Preoperative warm-up using a virtual reality simulator," *JSLS : Journal of the Society of Laparoendoscopic Surgeons*, vol. 15, no. 4, pp. 533–538, 2011.

[13] C. Bommer, S. Sullivan, K. Campbell, Z. Ahola, S. Agarwal, A. O'Rourke, H. S. Jung, A. Gibson, G. Leverson, and A. E. Liepert, "Pre-simulation orientation for medical trainees: An approach to decrease anxiety and improve confidence and performance," *American Journal of Surgery*, vol. 215, no. 2, pp. 266–271, 2018.

[14] A. Munawar, Y. Wang, R. Gondokaryono, and G. S. Fischer, "A real-time dynamic simulator and an associated front-end representation format for simulating complex robots and environments," pp. 1875–1882, 2019.

[15] K. Fan, A. Marzullo, N. Pasini, A. Rota, M. Pecorella, G. Ferrigno, and E. De Momi, "A unity-based da vinci robot simulator for surgical training," in *2022 9th IEEE RAS/EMBS International Conference for Biomedical Robotics and Biomechatronics (BioRob)*, 2022, pp. 1–6.

[16] J. M. Ferguson, B. Pitt, A. Kuntz, J. Granna, N. L. Kavoussi, N. Nimmagadda, E. J. Barth, S. D. Herrell, and R. J. Webster, "Comparing the accuracy of the da vinci xi and da vinci si for image guidance and automation," *International Journal of Medical Robotics and Computer Assisted Surgery*, vol. 16, no. 6, pp. 1–10, 2020.

[17] A. Herrel, A. Lowie, A. Miralles, P. Gaucher, N. J. Kley, J. Measey, and K. A. Tolley, "Burrowing in blindsnakes: A preliminary analysis of burrowing forces and consequences for the evolution of morphology," *The Anatomical Record*, vol. 304, no. 10, pp. 2292–2302, 2021.

[18] M. A. Adamo and I. F. Pollack, "A single-center experience with symptomatic postoperative calvarial growth restriction after extended strip craniectomy for sagittal craniosynostosis," *Journal of Neurosurgery: Pediatrics*, vol. 5, no. 1, pp. 131–135, 2010.

[19] A. Munawar, Z. Li, N. Nagururu, D. Trakimas, P. Kazanzides, R. H. Taylor, and F. X. Creighton, "Fully immersive virtual reality for skull-base surgery: surgical training and beyond," *International journal of computer assisted radiology and surgery*, vol. 19, no. 1, pp. 51–59, 2024.

[20] N. Rahman, N. J. Deaton, J. Sheng, S. S. Cheng, and J. P. Desai, "Modular fbg bending sensor for continuum neurosurgical robot," *IEEE Robotics and Automation Letters*, vol. 4, no. 2, pp. 1424–1430, 2019.

[21] P. J. Sincak, E. Prada, Miková, R. Mykhailyshyn, M. Varga, T. Merva, and I. Virgala, "Sensing of continuum robots: A review," *Sensors*, vol. 24, no. 4, p. 1311, 2024.

[22] D. Wei, H. Zhou, and H. Y. Yang, "Human-robot negotiation of intentions based on virtual fixtures for shared task execution," in *2020 17th International Conference on Ubiquitous Robots (UR)*, Kyoto, Japan, 2020, pp. 297–302.